INDERSCIENCE PUBLISHERS
Linking academia, business and industry through research

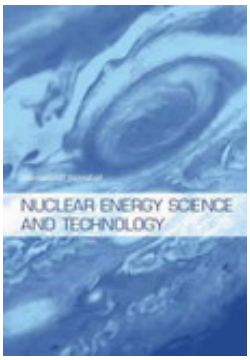

International Journal of Nuclear Energy Science and Technology

ISSN online: 1741-637X - ISSN print: 1741-6361
https://www.inderscience.com/ijnest

Spallation reaction study to improve cross-section measurements of fission products in nuclear waste using Cs-137 on proton or deuteron ranging from 0.1 to 2.4 GeV

Abdessamad Didi, Hamid Amsil, Hamid Bounouira, Khalid Laraki, Hamid Marah, Hassane Dekhissi, Mohamed Yjjou

DOI: 10.1504/IJNEST.2023.10058230

Article History:

Received:	04 November 2021
Last revised:	12 January 2022
Accepted:	11 February 2022
Published online:	07 August 2023

Spallation reaction study to improve cross-section measurements of fission products in nuclear waste using Cs-137 on proton or deuteron ranging from 0.1 to 2.4 GeV

Abdessamad Didi*, Hamid Amsil, Hamid Bounouira, Khalid Laraki and Hamid Marah

National Energy Center of Nuclear Science and Technology,
Rabat, Morocco
Email: a.didi@ump.ac.ma
Email: amsil@cnesten.org.ma
Email: bounouira@cnesten.org.ma
Email: laraki@cnesten.org.ma
Email: marah@cnesten.org.ma
*Corresponding author

Hassane Dekhissi and Mohamed Yjjou

Theoretical and Particles Physics and Modelling Laboratory (LPTPM),
Department of Physics,
Faculty of Sciences,
Mohammed Ist University,
Oujda, Morocco
Email: hdekhissi@yahoo.fr
Email: m.yjjou@ump.ac.ma

Abstract: The aim of this research was to study the spallation reaction of a cesium-137 target using a beam of protons or deuterons for the transmutation of nuclear waste, as well as to evaluate the differences in the production cross-section of the secondary spallation products, such as neutrons, protons, deuterons, pions (π^+, π^-, π_0), helions, tritons, and alphas. The work presented in this paper provides the necessary scientific evidence for confidently implementing the MCNP-calculated transmutation of cesium-137 using a spallation reaction. In our research we evaluated and improvised the different physical characteristics of the fission products of the cesium-137 target during a spallation reaction.

Keywords: transmutation; waste energy; spallation; cesium-137; MCNP; cross section; Monte Carlo.

Reference to this paper should be made as follows: Didi, A., Amsil, H., Bounouira, H., Laraki, K., Marah, H., Dekhissi, H. and Yjjou, M. (2023) 'Spallation reaction study to improve cross-section measurements of fission products in nuclear waste using Cs-137 on proton or deuteron ranging from 0.1 to 2.4 GeV', *Int. J. Nuclear Energy Science and Technology*, Vol. 16, No. 2, pp.67–79.

Biographical notes: Abdessamad Didi received his doctorate in Nuclear Physics and master's degree in the Nuclear Engineering from the University of Sidi Mohamed Ben Abdellah Fez, Morocco in 2013. He is currently a doctor in nuclear field at CNESTEN.

Hamid Amsil is currently researcher at the National Energy Center of Nuclear Science and Technology, Rabat, Morocco.

Hamid Bounouira is currently doctor researcher at the National Energy Center of Nuclear Science and Technology, Rabat, Morocco.

Khalid Laraki is currently Head of Analysis Unit at the National Energy Center of Nuclear Science and Technology, Rabat, Morocco.

Hamid Marah is currently scientific research director at the National Energy Center of Nuclear Science and Technology, Rabat, Morocco.

Hassane Dekhissi is currently a full Professor of Nuclear Physics and Head of the Theoretical and Particles Physics and Modelling Laboratory (LPTPM), Department of Physics, Faculty of Sciences at Mohammed Ist University in Oujda, Morocco. He works on neutronic, nuclear and particle physics, hadrontherapy, astrophysics, cosmic rays and medical physics.

Mohamed Yjjou is PhD student in Nuclear Physics at Mohamed 1st University in Oujda and has master's degrees in the Nuclear Engineering from the University of Sidi Mohamed Ben Abdellah Fez.

1 Introduction

Knowledge of nuclear reactions that are induced by high-energy heavy ions is essential for various fields, such as medicine (Didi et al., 2020a), space exploration (Tylka and Dietrich, 1999), research study (Didi et al., 2020b) and accelerator installation (Jin et al., 2015), whether for scientific research or the production of radioisotopes (Imal and Ogul, 2021). Indeed, in medical applications, ion beams with protons or heavier particles have become commonly used to treat cancer (Yan et al., 2020). Nuclear waste inevitably results, however, whether it is in the form of spent fuel itself or the waste resulting from its use, and without appropriate protection measures, this presents a high radiological risk for humans and the environment, possibly for a long period of time (Rajkhowa et al., 2021). This can persist for thousands of centuries due to the presence of actinides in some fission products. Transmutation therefore aims to convert long-lived radioactive elements into ones with a shorter life or stable elements (Kase et al., 1993). However, for cesium, the presence of various isotopes means that more long-lived elements are generated than destroyed, it is one of the many fission products of uranium and arguably the best known to have been used in hydrological and ecological studies following general atmospheric contamination induced, from 1945 onwards, through the use of atomic bombs and nuclear testing.

The three tools that have been studied for transmutation include thermal neutron reactors, fast-neutron reactors, and installations that couple a particle accelerator with a subcritical fast-neutron reactor (National Research Council, 1996).

The scientific feasibility of transmutation has been demonstrated, and evidence of technical feasibility now exists thanks to transmutation experiments in fast-neutron reactors (Wakabayashi et al., 2019). Unfortunately, the available data for transmutation is still insufficient for conducting a substantiated review of these technologies before starting to build prototype transmitter reactors. However, the results do offer several solutions for reducing the radiotoxicity of waste, thanks to fast-neutron reactors gradually replacing the current reactors in future with a 2040 horizon (IAEA, 2013).

2 Materials and methods

In this study, we looked at the distribution of the radioactive products that are formed when a cylindrical-shaped volume, with a diameter of 1 cm and a height of 1 cm, of cesium-137 is irradiated with beams of protons or deuterons with energies ranging from 100 MeV up to 2.4 GeV, with the target being placed in a 1 cm beam. Cesium was chosen due to it being mono-isotopic, because this makes it possible to establish specific reactions even when the reaction path is not known.

In our study, we chose to use MCNP6.1, which is the most widely used general purpose Monte Carlo neutron–photon–electron transport code for calculating the transport of particles and their interactions with matter (MCNP, 2014). As the name suggests, this system is based on the Monte Carlo method. The numerical simulation of a nuclear system also employs data libraries that contain the necessary information to calculate the radiation–matter interaction. Depending on the particular application, these data libraries may differ in their format or content, although they are usually built from a single ENDF/B-VII source (MCNP6, 2014).

Before we give our results, we will first mention the means that our research used to calculate the spectra of secondary particles and the cross sections of the products from the cesium-137 target, namely the LCA map from the input file for MCNP6.1 and the INXC69 GENXS option (Mashnik, 2014).

3 Results and discussion

A brief description of the current state of nuclear data for the nuclei most relevant to the transmutation of nuclear waste is required. In particular, this description should focus on the major deviations in the fission and capture cross sections of actinides, since these affect not only the transmutation rates but also the safety parameters of the system. For this, we used the cross-section data from the ENDF/B-VI library.

The effect, including the side reactions, was evaluated by the MCNP6.1 code in order to calculate the transport of particles and the nuclear reactions of a target bombarded by a 185 MeV beam of protons or deuterons. The configuration of the system being studied is illustrated in Figure 1, where the radius of the proton/deuteron beam was 1 cm and the length and diameter of the target were 1 cm. The beams of protons and deuterons were directly aimed at the target. The calculation's conditions and codes used are summarised in Table 1. The secondary neutron and proton fluxes were calculated radially and axially from the target, and the results of these calculations are shown in Figure 2.

Figure 1 Target prototype configuration using 185 MeV energy beams of protons/deuterons

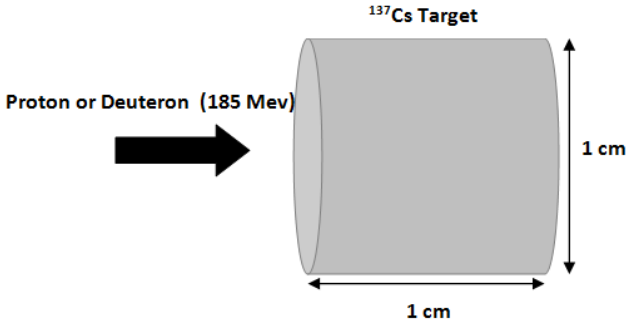

Table 1 Summary of calculations using MCNP6.1 code for 185 MeV energy beams of protons/deuterons

Type	*Proton*	*Deuteron*
Energy (MeV)	185	185
Height (cm)	1	1
Radius (cm)	0.5	0.5
Distance target-source (cm)	1	1
Genxs option	Inxc69	Inxc69
Total cross section (barn)	1.242	6.219
Neutron production cross section (barn	6.79	10.28
Neutron yield (n/p)	5.466	1.653
Proton production cross section (barn)	1.351	2.267
Proton yield (n/p)	1.087	0.3644
π^+ production cross section (barn)	6.66e-6	0
π^+ yield (n/p)	5.36e-6	0
π^- production cross section (barn)	8.04e-5	1.21e-8
π^- yield (n/p)	6.47e-5	1.29e-9
π_0 production cross section (barn)	2.41e-4	0
π_0 yield (n/p)	1.94e-4	0
Deuteron production cross section (barn)	0.197	0.067
Deuteron yield (n/p)	0.0925	0.0108
Triton production cross section (barn)	0.0925	0.0137
Triton yield (n/p)	0.0476	2.21e-3
Helion production cross section (barn)	0.023	6.45e-4
Helion yield (n/p)	0.0185	1.037e-4
Alpha production cross section (barn)	0.160	0.135
Alpha yield (n/p)	0.128	0.0216

Figure 2 shows the variation in the neutron and proton production cross sections as a function of particle spectra for incident particles in the ^{137}Cs target. Note that in Figure 2(a), the production of neutrons and secondary protons using a proton beam varies according to the energy of the incident particles, so production is more significant when the energy is greater. In addition, note that the production of these secondary particles (neutrons/protons) is almost identical when using the same incident energy.

Figure 2(b) shows the variation in the production of neutrons and protons when directing a deuteron beam of various energies at the ^{137}Cs target. Note that when the incident energy is greater, the production cross section for secondary particles is more significant, while the production of secondary particles (neutrons and protons), and is the same for each energy.

Figure 2 Neutron, proton spectrum production using 185 MeV proton beam (a) and 185 MeV deuterium beam (b) (see online version for colours)

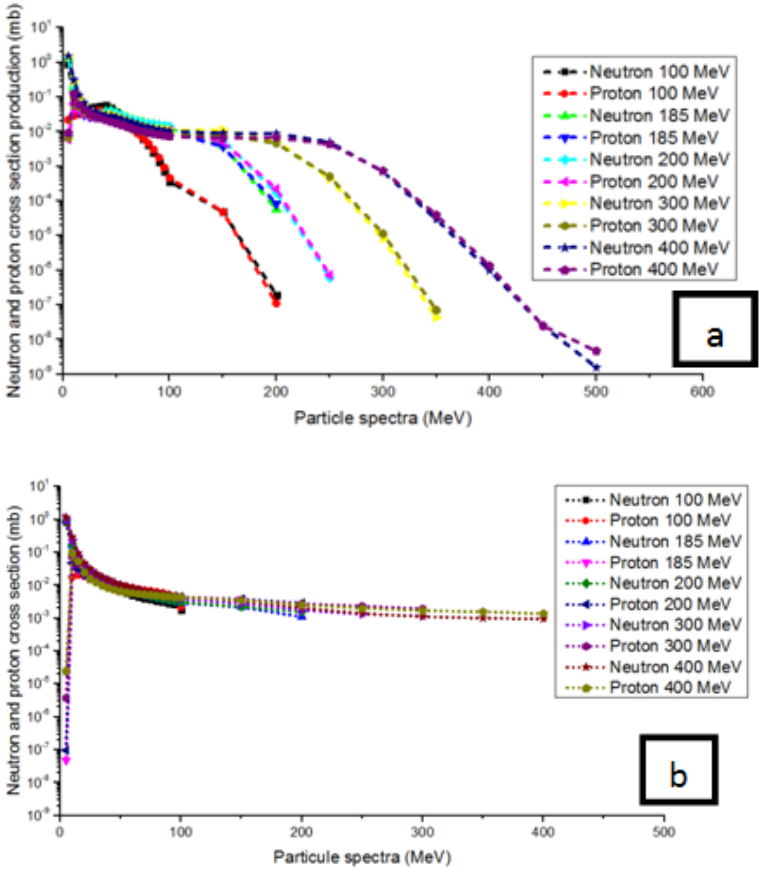

Theoretically, we can calculate the transmutation energy using the following formula (Kase et al., 1993), which calls for major transmutation factors, such as transmutation rate, which relates to the effective half-life and transmutation energy.

Starting with the average transmutation rate (Rate) in the volume region, which in our case is a cylinder with a 1 cm diameter and a height of 1 cm; this can be expressed as follows:

$$Rate_{t,r}(r) = \int \sigma(E,x)\varphi(E)\,dE \tag{1}$$

$$\overline{Rate}_{t,r}(r) = \frac{\iiint \lambda_{t,x}\,dx}{\iiint dx} \tag{2}$$

where x is the position of the waste nuclide in the target volume, E is the particle energy, $\sigma(E, x)$ is the cross section of relevant nuclear reaction, and $\varphi(E, x)$ is the proton or deuteron flux.

Thus, a relation between the transmutation rate and the number of target nuclides can be expressed as:

$$\frac{dN_t}{dt} = -\lambda_{nat}V_t - \overline{Rate}_{t,x}N_t \tag{3}$$

where λ_{nat} is the decay constant and N_t is the number of target nuclides.

Equation (4) then takes the following form:

$$N_t = N_0 e^{-\left(\lambda_{nat}+\overline{Rate}_{t,x}\right)t} \tag{4}$$

where N_0 represents the value of N_t at $t = 0$.

However, the transmutation energy E_t can be deduced from the primary energy of the beam by taking into account the transmutation of the target nuclide, and this can be explained by the following equation:

$$E_t = \frac{E_{particle}}{P(V)} \tag{5}$$

where $E_{particle}$ is the particle energy and $P(V)$ is the probability of a number of reactions being caused by the incident proton or deuteron beam in transmutation volume V.

However, we can deduce the reaction probability in equation (5) by taking into account the primary spallation reaction with the incident (proton/deuteron) beam.

$$P = 1 - e^{-N\sigma d} \tag{6}$$

where N is the atomic number density, representing the number of atoms of a given type per unit volume (cm^3) of the material, and d is the target's thickness.

The non-elastic cross section of the proton or deuteron beam is calculated by inserting the mass number M and the incident energy E, which must be greater than 20 MeV, using the following equation:

$$\sigma == 45M^{0.7}\left(1+0.016\sin\left(5.3-2.63\ln(M)\right)\right)\left(1-0.62e^{-\frac{E}{200}}\sin\left(10.9E^{-0.28}\right)\right) \tag{7}$$

This equation is a function of two parameters, M (mass number) and E (energy). To reduce equation (7), we can simplify it by using:

$$G = 1+0.016\sin\left(5.3-2.63\ln(M)\right) \text{ and } F = 1-0.62e^{-\frac{E}{200}}\sin\left(10.9E^{-0.28}\right)$$

Finally, through approximation, we derive the following empirical transmutation equation:

$$\sigma = 45M^{0.7} f(G) f(F)$$

In this part of the work, we used the MCNP6.1 code to calculate the total production cross sections of secondary particles produced by spallation reactions when using proton and deuteron beams with energies between 0.1 and 2.4 GeV aimed at a ^{137}Cs target, and Table 2 summarises the results of this.

When analysing Table 2, note the slight difference in results when using a proton or deuteron beam.

Table 2 Summary of calculations using MCNP6.1 code proton and deuteron beams with energies between 0.1 and 2.4 GeV aimed at a ^{137}Cs target

Energy	*Beam*	*n*	*p*	π^+	π^-	π_0	*d*	*T*	*H*	*a*
100	D	7,249	1,973	0,000	0,000	0,000	0,067	0,001	0,000	0,019
	P	5,476	0,990	0,000	0,000	0,000	0,111	0,024	0,010	0,056
200	D	10,600	2,347	0,000	0,000	0,000	0,077	0,017	0,001	0,159
	P	7,024	1,414	0,000	0,000	0,001	0,212	0,066	0,025	0,178
300	D	12,010	2,887	0,000	0,000	0,000	0,138	0,042	0,003	0,271
	P	8,402	1,870	0,003	0,004	0,009	0,335	0,087	0,026	0,206
400	D	12,900	3,332	0,000	0,000	0,000	0,186	0,062	0,005	0,326
	P	9,427	2,032	0,016	0,017	0,038	0,586	0,174	0,054	0,836
500	D	13,640	3,710	0,001	0,002	0,003	0,261	0,078	0,007	0,662
	P	10,360	2,296	0,039	0,037	0,083	0,736	0,226	0,071	0,359
600	D	14,360	4,069	0,004	0,009	0,010	0,265	0,094	0,009	0,405
	P	11,670	2,659	0,070	0,066	0,137	0,933	0,294	0,094	0,461
700	D	15,160	4,442	0,010	0,023	0,026	0,311	0,131	0,011	0,452
	P	12,920	3,040	0,108	0,097	0,190	1,145	0,366	0,120	0,571
800	D	16,060	4,850	0,022	0,044	0,050	0,364	0,134	0,015	0,506
	P	14,050	3,422	0,131	0,132	0,240	1,360	0,440	0,148	0,684
900	D	17,040	5,295	0,039	0,073	0,082	0,430	0,158	0,002	0,570
	P	15,060	3,790	0,161	0,170	0,291	1,576	0,513	0,177	0,796
1000	D	18,020	5,750	0,060	0,106	0,119	0,500	0,185	0,025	0,638
	P	15,960	4,148	0,189	0,207	0,342	1,788	0,584	0,207	0,905
1100	D	19,020	6,220	0,083	0,142	0,158	0,576	0,214	0,031	0,707
	P	17,360	5,013	0,217	0,243	0,390	1,753	0,553	0,207	0,949
1200	D	19,940	6,680	0,107	0,178	0,200	0,655	0,242	0,038	0,774
	P	18,110	5,365	0,241	0,276	0,436	1,947	0,615	0,235	1,040
1300	D	20,800	7,115	0,131	0,214	0,238	0,729	0,270	0,045	0,837
	P	18,790	5,700	0,264	0,308	0,478	2,138	0,677	0,264	1,126

Table 2 Summary of calculations using MCNP6.1 code proton and deuteron beams with energies between 0.1 and 2.4 GeV aimed at a ^{137}Cs target (continued)

Energy	*Beam*	*n*	*p*	π^+	π^-	π_0	*d*	*T*	*H*	*a*
1400	D	21,570	7,510	0,153	0,248	0,276	0,801	0,290	0,052	0,895
	P	18,790	5,700	0,264	0,308	0,478	2,138	0,677	0,264	1,126
1500	D	22,250	7,880	0,175	0,278	0,311	0,869	0,323	0,059	0,947
	P	20,000	6,330	0,306	0,366	0,558	2,515	0,795	0,322	1,282
1600	D	22,850	8,220	0,195	0,309	0,344	0,935	0,347	0,066	0,994
	P	20,550	6,628	0,327	0,393	0,597	2,700	0,850	0,352	1,350
1700	D	23,390	8,530	0,214	0,337	0,374	0,998	0,371	0,073	1,037
	P	21,080	6,924	0,348	0,420	0,634	2,883	0,906	0,381	1,419
1800	D	23,860	8,810	0,231	0,362	0,403	1,054	0,392	0,080	1,073
	P	21,600	7,214	0,369	0,446	0,671	3,066	0,959	0,411	1,480
1900	D	17,860	5,430	0,386	0,591	0,682	1,691	0,506	0,175	0,769
	P	22,110	7,504	0,390	0,471	0,707	3,249	1,012	0,441	1,539
2000	D	18,250	5,630	0,413	0,625	0,726	1,771	0,532	0,185	0,801
	P	22,620	7,791	0,411	0,496	0,744	3,431	1,064	0,470	1,596
2100	D	18,610	5,810	0,440	0,661	0,768	1,852	0,558	0,195	0,834
	P	23,110	8,074	0,432	0,521	0,780	3,616	1,115	0,501	1,649
2200	D	18,940	5,980	0,468	0,695	0,811	1,928	0,582	0,205	0,862
	P	23,610	8,357	0,452	0,547	0,816	3,801	1,163	0,530	1,700
4300	D	19,260	6,140	0,494	0,731	0,852	2,000	0,607	0,214	0,893
	P	24,410	8,643	0,472	0,574	0,853	3,956	1,213	0,561	1,750
2400	D	19,560	6,300	0,522	0,766	0,893	2,075	0,628	0,224	0,923
	P	24,600	8,925	0,493	0,601	0,891	4,173	1,263	0,591	1,797

Recent experimental and theoretical data for the yield of spallation and fission products for a cesium-137 target being irradiated by a 185 MeV beam of protons or deuterons were compared with the results of the MCNP code calculations in this study, and these are illustrated in Figure 3 (Wang et al., 2016; Yang et al., 2019). The production cross-section for the spallation residues (^{49}In, ^{50}Sn) that were calculated with the MCNP6.1 code with a 185 MeV proton or deuteron beam bombarding the ^{137}Cs target are represented in the form of isotopic distributions.

To validate our results, we avoided excessively complex plots and selected experimental data that was already available in previously published articles (Mashnik, 2014; Wang et al., 2016). Most of the curves have a Gaussian-like shape, and the isotopes produced in Figures 4(a) to 4(f) are ^{51}Sb, ^{52}Te, ^{53}I, ^{54}Xe, ^{55}Cs and ^{56}Ba. The curves in black and red represent our results, while the validation curves are colored green, pink, blue, and dark blue.

On analysing the data in Figure 4, it becomes clear that all the presented distributions are compatible with the characteristic Gaussian distribution curve. The isotopes' production cross sections vary from one to another, however.

Figure 3 Production cross sections for In ($Z = 49$) and Sn ($Z = 50$) using a 185 MeV beam of protons/deuterons

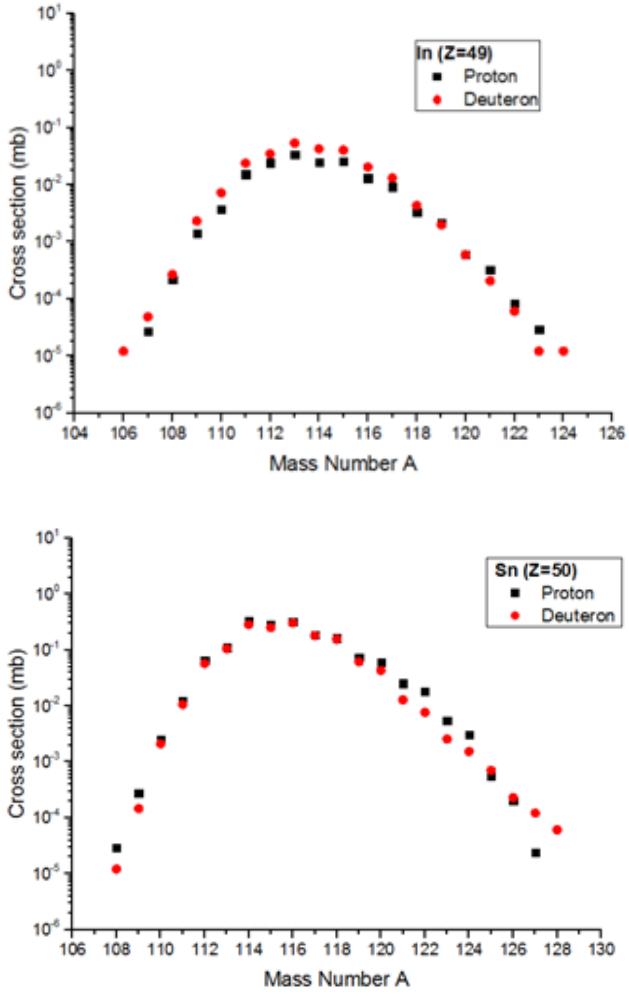

Calculations were performed using different chart templates. In addition, evaporation and fission models are presented in Figure 4 with the corresponding experimental data.

The agreement between the calculated and experimental data clearly reveals there is a more precise estimation of the associated model parameters. For example, to improve the description of the fission fragments yields with MCNP, it is necessary to use a GENXS option, so for our research, we used the INXC69 package for the mass distribution of the fission fragments in order to obtain a coherent description of the observed fission cross sections. The results of this are shown in Figure 4, where the experimental data available for the cross section of Cesium fission are also presented.

The experimental results are in agreement with the results of the MCNP code (Mashnik, 2014; Wang et al., 2016). For the transport of protons with beam energies less than 150 MeV, cross-section data implemented in MCNP6.1 were used with the cascade-exciton model CEM 03.03 to simulate the interactions of nucleons, while for beams with energies greater than 150 MeV, we used the LAQGSM 03.03 package.

Figure 4 Mass distribution of cesium-137 isotopes produced under proton (e) and deuteron (f) bombardment at 185 MeV (see online version for colours)

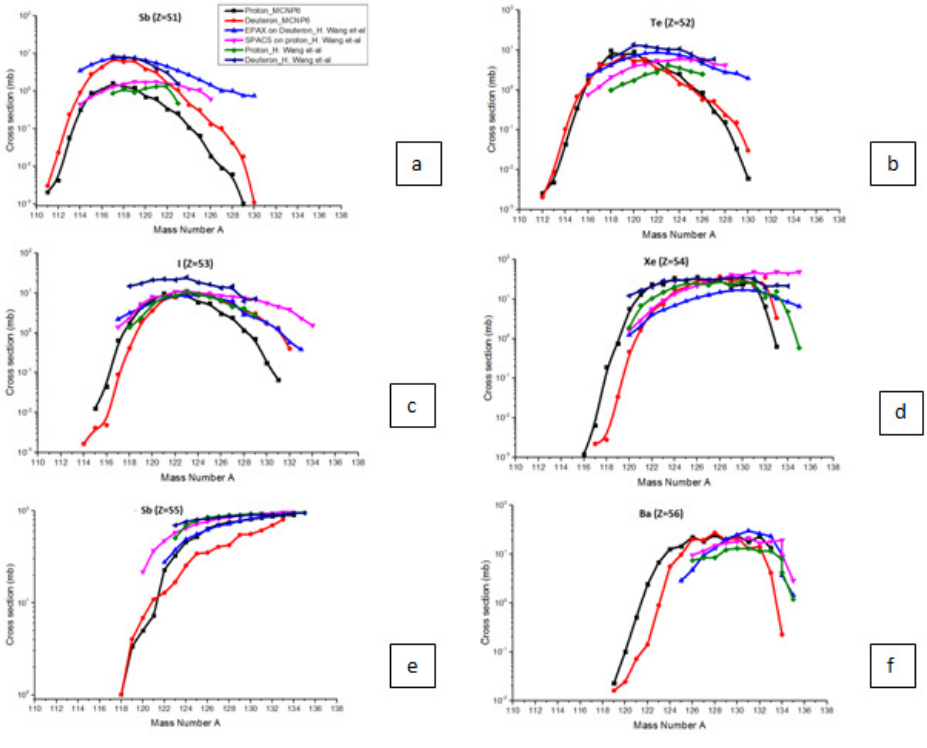

The two packages, CEM and LAQGSM, are able to deal with fragmentation reactions induced by nucleons and the nucleus, and they take into account all the stages of a nuclear reaction, namely intranuclear cascade and pre-equilibrium decay followed by evaporation and equilibrium fission of compound nuclei.

Figure 5 shows the variation in the production cross section with a 185 MeV beam of protons (black curve) and deuterons (red curve). The curves for protons and deuterons are very similar, with just a small difference in the physical nature of the output cross section in the vapourisation range between $A = 5$ and $A = 35$, while the fission products from $A = 35$ to $A = 100$ are most efficient with the proton beam.

Figure 5 Distribution of 185 MeV using protons beams and deuterons beams

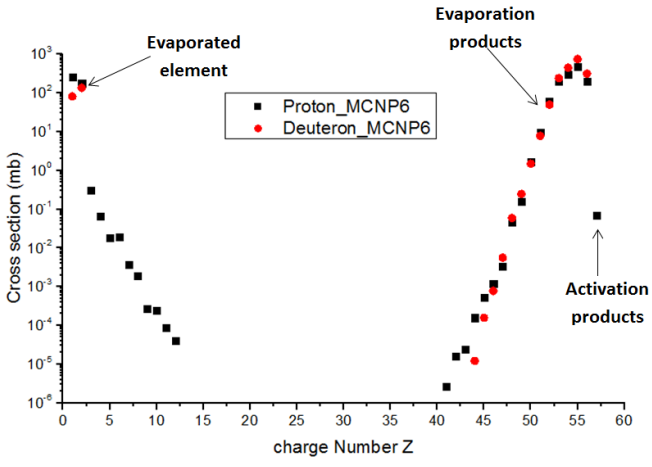

In the subsequent part of this study, we were interested in simulating residual mass number products by varying the energy of the proton and deuteron beams between 0.1 GeV and 2.4 GeV, with Figures 6 and 7 illustrating the results of this.

The cross section distribution of the spallation products indicates a variation in the levels of mass production obtained when using ^{137}Cs. Note that when the energy exceeds 1 GeV, four physical phenomena appear in the form of the evaporation of elements, the appearance of fission products, the evaporation of these products, and activation of the products. On the other hand, when the energy of the beams is less than 1 GeV there are only three phenomena, namely the evaporation of elements, the evaporation of products, and the activation of products.

Figure 6 Simulation data for spallation production of residual-mass number (A) using proton beams of 0.1, 0.5, 1, 1.5, 2 and 2.4 GeV with a ^{137}Cs target

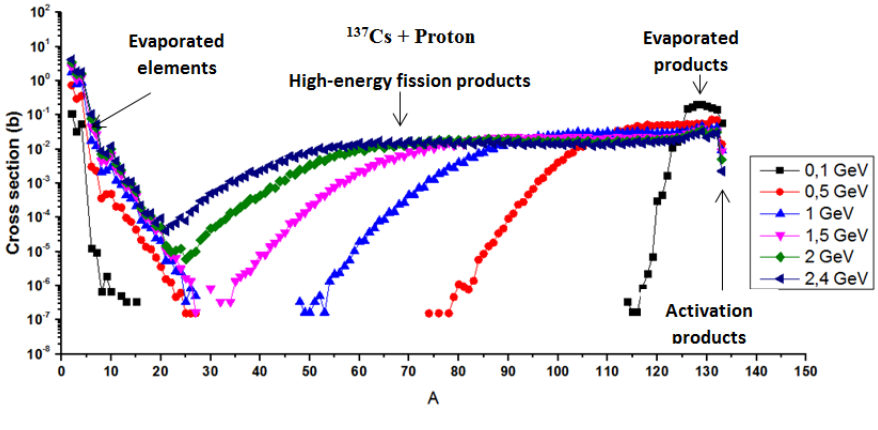

Figure 7 Simulation data for spallation production of residual-mass number (A) using deuterium beams of 0.1, 0.5, 1, 1.5, 2 and 2.4 GeV with a ^{137}Cs target

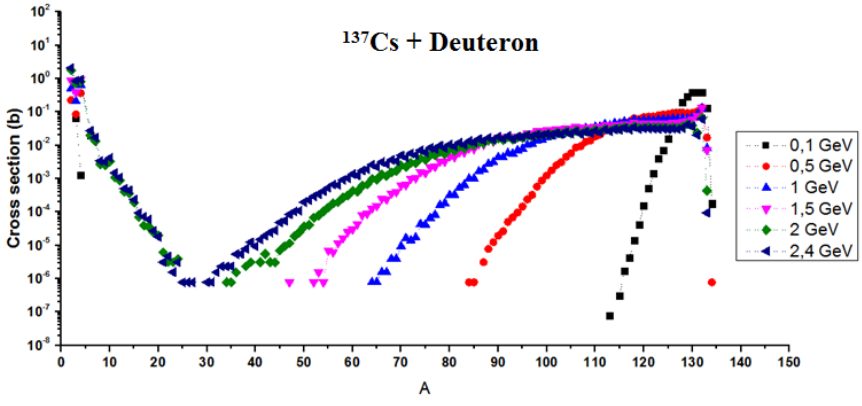

4 Conclusion

The purpose of this research was to provide more knowledge about the transmutation of cesium-137, a fission product produced in nuclear reactors and to verify spallation reaction as an effective means for converting the radiotoxicity of this material from a long-lasting one to a short-lasting one.

We therefore verified recent simulation data using MCNP6.1 code for the yields of spallation and fission products for a ^{137}Cs target when irradiating it with proton or deuteron beams with energies between 100 MeV and 2.4 GeV. The code's results gave ample data to essentially improve the accuracy of our knowledge of targeting ^{137}Cs as a radioactive element.

References

Didi, A. et al. (2020a) 'Helium ion therapy compared to protons therapy using MCNP Monte-Carlo code', *Physics AUC*, Vol. 30, pp.16–23.

Didi, A., Dekhissi, H., Dadouch, A., Bencheikh, M. and Sebihi, R. (2020b) 'New study of spallation reactions (Be + p) and (Sn + p) at 1.2 GeV per nucleon', *Journal of King Saud University - Science*, Vol. 32, No. 3, pp.2163–2169.

IAEA (2013) 'Fast reactors and related fuel cycles: safe technologies and sustainable scenarios', *Proceedings of an International Conference*, Paris, France, 4–7 March.

Imal, H. and Ogul, R. (2021) 'Theoretical study of isotope production in the peripheral heavy-ion collision 136Xe + Pb at 1 GeV/nucleon', *Nuclear Physics A*, Vol. 1014.

Jin, H., Jang, J., Jang, H. and Jeon, D. (2015) 'Lattice design and beam dynamics studies of the high energy beam transport line in the RAON heavy ion accelerator', *Nuclear Instruments and Methods in Physics Research Section A: Accelerators, Spectrometers, Detectors and Associated Equipment*, Vol. 802, pp.67–75.

Kase, T., Konashi, K., Takahashi, H. and Hirao, Y. (1993) 'Transmutation of Cesium-137 using proton accelerator', *Journal of Nuclear Science and Technology*, Vol. 30, No. 9, pp.911–918.

Mashnik, S.G. (2014) *V&V of MCNP 6.1.1 Beta Against Intermediate and High-Energy Experimental Data, The MCNP6 Code Package, LA-UR-14-27018*.

MCNP (2014) *Monte Carlo Team X-6, N-Particle Transport Code System Including MCNP6.1*.

MCNP6 (2014) *Data Libraries, MCNP6 User's Manual, Code Version 6.1.1beta, LA-CP-14-00745*, Los Alamos National Security, LLC.

National Research Council (1996) *Nuclear Wastes: Technologies for Separations and Transmutation*, The National Academies Press, Washington, DC, https://doi.org/10.17226/4912.

Rajkhowa, S., Sarma, J. and Das, A.R. (2021) 'Radiological contaminants in water: pollution, health risk, and treatment', in Ahamad, A., Siddiqui, S.I. and Singh, P. (Eds): *Contamination of Water*, Academic Press, pp.217–236.

Tylka, A.J. and Dietrich, W.F. (1999) 'IMP-8 observations of the spectra, composition, and variability of solar heavy ions at high energies relevant to manned space missions', *Radiation Measurements*, Vol. 30, No. 3, pp.345–359.

Wakabayashi, T., Tachi, Y., Takahashi, M. et al. (2019) 'Study on method to achieve high transmutation of LLFP using fast reactor', *Sci Rep*, Vol. 9.

Wang, H. et al. (2016) 'Spallation reaction study for fission products in nuclear waste: cross section measurements for 137Cs and 90Sr on proton and deuteron', *Physics Letters B*, Vol. 754, pp.104–108.

Yan, J.W. et al. (2020) 'Prototype design of readout electronics for In-Beam TOF-PET of Heavy-Ion Cancer Therapy Device', *Nuclear Instruments and Methods in Physics Research Section A: Accelerators, Spectrometers, Detectors and Associated Equipment*, Vol. 959.

Yang, G., Xu, S., Jin, M. and Su, J. (2019) 'Prediction of the cross-sections of isotopes produced in deuteron-induced spallation of long-lived fission products', *Chinese Phys. C*, Vol. 43.